Porous Anatase Nanoparticles with High Specific Surface Area Prepared by Miniemulsion Technique

Renate Rossmanith,[†] Clemens K. Weiss,[†] Jasmin Geserick,[‡] Nicola Hüsing,[‡] Ute Hörmann,[§] Ute Kaiser,[§] and Katharina Landfester*[,†,||]

Institute of Organic Chemistry III/Macromolecular Chemistry and Organic Materials, Institute of Inorganic Chemistry I, and Central Facility of Electron Microscopy, Ulm University, 89081 Ulm, Germany, and Max Planck Institute for Polymer Research, Ackermannweg 10, 55128 Mainz, Germany

Received February 22, 2008. Revised Manuscript Received June 25, 2008

A simple template-free approach to generate spherical porous anatase nanoparticles by combining the sol−gel process with the inverse miniemulsion technique is reported. These as-synthesized particles of about 200 nm in diameter consist of aggregated small anatase crystallites of several nanometers, thus leading to a high specific surface area of more than 300 $m^2 \cdot g^{-1}$, even after calcination at 400 °C. The only employed surfactant is a block copolymer (P(E/B-b-EO)), which stabilizes the aqueous droplets with the water-soluble precursor bis(2-hydroxyethyl)titanate (EGMT) in the organic phase but also leads to aggregation and pore formation inside the particles. The lower relative rates of hydrolysis and condensation compared to the commonly used titanium alkoxides allow convenient handling in miniemulsion. Here we report the effects of synthesis conditions, such as the amount of surfactant, the composition of the dispersed phase, and the reaction and calcination temperature, on the particle size, porosity, crystallite size, crystallite phase, and specific surface area of the obtained nanoparticulate material. After removing the continuous phase, the obtained powders were characterized before and after calcination by transmission (TEM) and scanning electron microscopy (SEM), X-ray diffraction (XRD), and nitrogen sorption (BET).

Introduction

Titanium dioxide is one of the most studied oxides due to its high photocatalytic activity[1] and interesting electrochemical properties.[2] It is of great interest in various applications, for example, in the fabrication of solar cells,[3] in photocatalysis,[1] and as electrodes in lithium batteries[4] and white pigments.[5] Its chemical stability, the high refraction index (n_D = 2.55−2.75 (anatase) and 2.7−3.1 (rutile)), the high ultraviolet absorptivity,[6] and the low costs are the main properties that make this material so interesting. Specifically, the preparation of spherical mesoporous TiO_2 particles (particles with pores between 2 and 50 nm) has attracted great attention because of their large surface area, thus finding application in chromatography,[7] bioseparation,[8] and nanotechnology.[9] Generally, stable mesostructures allow the rapid diffusion during photocatalytic reactions, consequently enhancing the reaction speed and therefore offering more active sites for adsorption. For these applications, a control over the crystal phase, particle size, particle size distribution, and porosity of the material is important for adjusting the coupled chemical and physical properties such as the specific surface area, the chemical reactivity, and the stability.[10]

Titanium dioxide occurs mainly in three crystalline phases: anatase, rutile, and brookite, which differ in their physical properties, such as the refractive index, dielectric constant, and chemical and photochemical reactivity. Rutile is the thermodynamically stable phase at standard pressure and normal temperatures; however, because of its larger band gap, anatase is the preferred polymorph for solar cells and in photocatalysis.[11]

Many methods have been established for generating colloidal anatase particles. Among all techniques the sol−gel approach is of particular interest, which includes the controlled hydrolysis and condensation of appropriate precursors, mostly titanium alkoxides. There are several factors that affect the sol−gel process and thus the resulting material such as the reactivity of the precursor, the pH of the reaction medium, the water to precursor ratio, and the reaction

* Prof. Dr. Katharina Landfester email: landfester@mpip-mainz.mpg.de phone: 0049-6131-379-170; fax:0049-6131-379-370
[†] Institute of Organic Chemistry III/Macromolecular Chemistry and Organic Materials, Ulm University.
[‡] Institute of Inorganic Chemistry I, Ulm University.
[§] Central Facility of Electron Microscopy, Ulm University.
[||] Max Planck Institute for Polymer Research.

(1) Zhang, Z.; Wang, C.; Zakaria, R.; Ying, Y. *J. Phys. Chem. B* **1998**, *102*, 10871.
(2) Fukushima, K.; Yamada, I. *J. Appl. Phys.* **1989**, *65*, 619.
(3) Park, N. G.; van de Lagemaat, J.; Frank, A. J. *J. Phys. Chem. B* **2000**, *104*, 8989.
(4) Kavan, L.; Gratzel, M.; Rathousky, J.; Zukalb, A. *J. Electrochem. Soc.* **1996**, *143*, 394.
(5) Hsu, W. P.; Yu, R.; Matijevic, E. *J. Colloid Interface Sci.* **1993**, *156*, 56.
(6) Wang, R.; Hashimoto, K.; Fujishima, A.; Chikuni, M.; Kojima, E.; Kitamura, A.; Shimohigoshi, M.; Watanabe, T. *Adv. Mater.* **1998**, *10*, 135.
(7) Jiang, Z. T.; Zuo, Y. M. *Anal. Chem.* **2001**, *73*, 686.
(8) Ye, L.; Pelton, R.; Brook, M. A. *Langmuir* **2007**, *23*, 5630.
(9) Lu, Y.; Fan, H.; Stump, A.; Ward, T. L.; Rieker, T.; Brinker, C. J. *Nature* **1999**, *398*, 223.
(10) Wang, W.; Gu, B.; Liang, L.; Hamilton, W. A.; Wesolowski, D. J. *J. Phys. Chem. B* **2004**, *108*, 14789.
(11) Zhang, H.; Banfield, J. F. *J. Mater. Chem.* **1998**, *8*, 2073.

10.1021/cm800533a CCC: $40.75
Published on Web 08/26/2008

temperature.[12] Usually, the precipitates obtained by sol−gel processing are porous but amorphous.[12] To induce a transition from the amorphous to the anatase phase, generally an annealing temperature higher than 300 °C is required leading to a collapse of the pore system and an increase of the particle size.

Anatase nanoparticles with special morphologies were prepared by Chemseddine and Moritz using organic ligands as stabilizing agents by means of wet chemistry.[13] Titania spheres between 500 and 700 nm were synthesized by Jiang et al. and Pal et al. through slow hydrolysis of titanium glycolate precursors.[14,15] However, the as-synthesized particles were amorphous and had to be annealed; moreover, the particles were synthesized in a solution with an extremely diluted titanium precursor concentration (<0.077 M).

There are only a few groups that reported the synthesis of crystalline titania at temperatures below 100 °C.[16−24] However, in most cases the obtained materials display no porosity or high specific surface areas. Kim et al.,[25] for example, synthesized a crystalline material below 100 °C, with quite large anatase particles (2−5 μm) consisting of 10 nm primary particles and a specific surface area not exceeding 148 $m^2 \cdot g^{-1}$.

When the sol−gel process is combined with the principles of liquid crystal-templating, mesoporous materials can be synthesized. One of the major problems in the synthesis of mesoporous titania is the balance between the hydrolysis−condensation processes on the one hand and the self-assembling reactions on the other. By optimizing the precursor chemistry and processing conditions, materials with different microstructure and surface chemistry can be obtained.

In 1995, Antonelli and Ying first synthesized hexagonally organized mesoporous titania by a modified sol−gel synthesis using alkyl phosphate surfactants and titanium isopropoxide bisacetylacetonate as precursor;[26] however, it was not pure titania due to incorporation of phosphorus from the template, thus limiting the use as catalyst. Mesoporous phosphorus-free titania was later prepared by the same group[27] using dodecylamine as template, which was then removed by extraction. These materials had a high specific surface area of 700 $m^2 \cdot g^{-1}$, but they were not thermally stable; after calcination a specific surface area of only about 50 $m^2 \cdot g^{-1}$ was found. In recent years, the synthesis of mesoporous TiO_2 under many different conditions has been extensively studied. Different synthetic methods have been developed with a variety of templates, such as alkyl phosphate anionic surfactants,[26] quaternary ammonium cationic templates,[16,17,28−33] primary amines,[27,34−36] and poly(ethylene oxide)-based surfactants[33,37−40] or nonsurfactant templates.[41] The most striking example was reported by Yang et al.[37] who reported thermally stable and large-pore mesoporous titania by using amphiphilic poly(alkylene oxide) block copolymers as structure-directing agents and inorganic titanium salts in a nonaqueous (ethanol) solution. However, this synthesis is time-consuming and leads only to low structural regularity.

In summary, most reported syntheses result in anatase with very low thermal stability. Upon calcination the structural order and surface area is drastically reduced. Only in mesoporous large-pore titania directed with poly(ethylene oxide)-based templates could higher temperatures up to 400 °C be applied without collapse of the mesophase.[37,38]

However, it is known that the photocatalytic activity of anatase increases with smaller particle size, high porosity, high specific surface area, and high degree of crystallinity.[32] Therefore, finding a technique to obtain pure anatase at low processing temperature with both small grain size and a high degree of crystallinity is still a challenge.

The miniemulsion process is a very suited technique which would enable the transformation of monodisperse stable droplets into TiO_2 nanoparticles. A miniemulsion consists of two immiscible liquids, a surfactant which prevents droplet collision and coalescence, and a special additive as osmotic pressure agent which is soluble in the dispersed phase and extremely insoluble in the continuous phase, thus suppressing Ostwald ripening by producing an osmotic pressure.[42] The two phases are homogenized by ultrasonication. Unlike a microemulsion in which diffusion processes take place

(12) Wang, C. C.; Ying, J. Y. *Chem. Mater.* **1999**, *11*, 3113.
(13) Chemseddine, A.; Moritz, T. *Eur. J. Inorg. Chem.* **1999**, *1999*, 235.
(14) Pal, M.; GarciaSerrano, J.; Santiago, P.; Pal, U. *J. Phys. Chem. C* **2007**, *111*, 96.
(15) Jiang, X.; Herricks, T.; Xia, Y. *Adv. Mater.* **2003**, *15*, 1205.
(16) Shibata, H.; Ogura, T.; Mukai, T.; Ohkubo, T.; Sakai, H.; Abe, M. *J. Am. Chem. Soc.* **2005**, *127*, 16396.
(17) Shibata, H.; Mihara, H.; Mukai, T.; Ogura, T.; Kohno, H.; Ohkubo, T.; Sakai, H.; Abe, M. *Chem. Mater.* **2006**, *18*, 2256.
(18) Testino, A.; Bellobono, I. R.; Buscaglia, V.; Canevali, C.; D'Arienzo, M.; Polizzi, S.; Scotti, R.; Morazzoni, F. *J. Am. Chem. Soc.* **2007**, *129*, 3564.
(19) Xu, J.; Liping, L.; Yan, Y.; Wang, H.; Wang, X.; Fu, X.; Li, G. *J. Colloid Interface Sci.* **2008**, *318*, 29.
(20) Mahshid, S.; Askari, M.; Ghamsari, M. S. *J. Mater. Process. Technol.* **2007**, *189*, 296.
(21) Liu, H.; Yang, W.; Ma, Y.; Cao, Y.; Yao, J.; Zhang, J.; Hu, T. *Langmuir* **2003**, *19*, 3001.
(22) Zhang, H.; Banfield, J. F. *Chem. Mater.* **2002**, *14*, 4145.
(23) Morales, B. A.; Novaro, O.; López, T.; Sánchez, E.; Gómez, R. *Mater. Res. Soc.* **1995**, *10*, 2788.
(24) Matijevic, E.; Budnik, M.; Meites, L. *J. Colloid Interface Sci.* **1977**, *61*, 302.
(25) Kim, S.-J.; Park, S.-D.; Jeong, Y. H. *J. Am. Ceram. Soc.* **1999**, *82*, 927.
(26) Antonelli, D. M.; Ying, J. Y. *Angew. Chem. Int. Ed. Engl.* **1995**, *34*, 2014.
(27) Antonelli, D. M. *Microporous Mesoporous Mater.* **1999**, *30*, 315.
(28) On, D. T. *Langmuir* **1999**, *15*, 8561.
(29) Blanchard, J.; Schuth, F.; Trens, P.; Hudson, M. *Microporous Mesoporous Mater.* **2000**, *39*, 163.
(30) Cabrera, S.; El Haskouri, J.; Beltran-Porter, A.; Beltran-Porter, D.; Marcos, M. D.; Amoros, P. *Solid State Sci.* **2000**, *2*, 513.
(31) Soler-Illia, G. J. d. A. A.; Louis, A.; Sanchez, C. *Chem. Mater.* **2002**, *14*, 750.
(32) Peng, T.; Zhao, D.; Dai, K.; Shi, W.; Hirao, K. *J. Phys. Chem. B* **2005**, *109*, 4947.
(33) Alvaro, M.; Aprile, C.; Benitez, M.; Carbonell, E.; Garcia, H. *J. Phys. Chem. B* **2006**, *110*, 6661.
(34) Wang, Y.; Chen, S.; Tang, X.; Palchik, O.; Zaban, A.; Koltypin, Y.; Gedanken, A. *J. Mater. Chem.* **2001**, *11*, 521.
(35) Yoshitake, H.; Sugihara, T.; Tatsumi, T. *Chem. Mater.* **2002**, *14*, 1023.
(36) Cassiers, K.; Linssen, T.; Mathieu, M.; Bai, Y. Q.; Zhu, H. Y.; Cool, P.; Vansant, E. F. *J. Phys. Chem. B* **2004**, *108*, 3713.
(37) Yang, P.; Zhao, D.; Margolese, D. I.; Chmelka, B. F.; Stucky, G. D. *Nature* **1998**, *396*, 152.
(38) Yang, P.; Zhao, D.; Margolese, D. I.; Chmelka, B. F.; Stucky, G. D. *Chem. Mater.* **1999**, *11*, 2813.
(39) Kluson, P.; Kacer, P.; Cajthaml, T.; Kalaji, M. *J. Mater. Chem.* **2001**, *11*, 644.
(40) Yu, J. C.; Zhang, L.; Yu, J. *Chem. Mater.* **2002**, *14*, 4647.
(41) Saadoun, L.; Ayllon, J. A.; Jimenez-Becerril, J.; Peral, J.; Domenech, X.; Rodriguez-Clemente, R. *Appl. Catal. B* **1999**, *21*, 269.
(42) Landfester, K. *Annu. Rev. Mater. Res.* **2006**, *36*, 231.

leading to an exchange of reactants, a miniemulsion is stabilized against diffusion and critically stabilized against coalescence and collision. During hydrolysis and condensation each droplet acts as a nanoreactor under preservation of droplet size, droplet number, and concentration in each droplet. Thus the final particle size can be easily tuned by the droplet size. Very recently Zhang et al.[43] published a synthesis of anatase nanoparticles of about 15 nm applying the inverse miniemulsion technique with tetrabutyltitanate as precursor. However, the as-synthesized particles are amorphous in nature and phase transition to anatase is only induced after thermal treatment at 550 °C. Moreover, the particles are not porous, consequently the highest specific surface area obtained is only about 170 $m^2 \cdot g^{-1}$. This is probably due to the fast condensation reaction of the precursor material.

As the relative rates of hydrolysis and polycondensation are known to strongly influence the structure and properties of the resulting metal oxides,[39] it is desirable to slow down this process as much as possible. In the case of the most commonly used titanium alkoxide for the sol−gel process such as titanium (IV) isopropoxide or other titanium alkoxides, hydrolysis and condensation start immediately in the presence of water (even on contact with moisture).[15] Therefore a new class of glycol-modified precursors was established which are more resistant to hydrolysis and can be kept in air for several weeks without observing any reaction. Another advantage of these glycol-modified precursors is their water solubility in acidic medium. This is particularly important for preparing mesoporous materials by templating of an aqueous liquid crystalline phase. With the use of the glycol-modified titanate the structuring surfactant can be directly dissolved in the aqueous phase without the addition of a cosolvent such as ethanol. Nevertheless, there are only few reports concerning the use of 1,2-diolates as precursor for the preparation of titania.[14,15,41,44,45]

To obtain small crystalline anatase nanoparticles by a slow and therefore controlled formation process, we combine the inverse miniemulsion technique with the sol−gel process using bis(2-hydroxyethyl)titanate (EGMT) as precursor material in high concentration. This novel template-free approach leads to porous anatase nanoparticles of controlled size and high specific surface area. As a result of the lower relative rates of hydrolysis and condensation, a convenient handling in miniemulsion is observed resulting in particles which are built up of small anatase crystallites of several nanometers which aggregate and form spherical particles with an average size of about 200 nm. The obtained porous anatase nanoparticles have a specific surface area of more than 300 $m^2 \cdot g^{-1}$ without using additional templates in the dispersed aqueous phase. The amount of the employed surfactant block copolymer (P(E/B-b-EO)) allows one to control the crystallite size and consequently the specific surface area. Since anatase is formed directly in miniemulsion, for crystallization no thermal treatment is necessary. After calcination at 400 °C, the high specific surface area can be preserved. The effect of synthesis conditions such as the amount of surfactant, composition of the dispersed phase, and the reaction and calcination temperature on particle size, porosity, crystallite size, crystallite phase, and specific surface area was investigated.

Table 1. Recipe for Preparation of TiO_2 Nanoparticles by Inverse Miniemulsion Technique

ingredient	amount
EGMT	313 mg
HCl (1 M)	2−10 mL
EG	0−8 mL
P(E/B-b-EO)	0.7−5 wt % (with respect to the dispersed phase)
Isopar M	25 g

Experimental Section

Materials. Tetrahydrofuran (THF) (Merck, 99.8%) was distilled over sodium hydride prior to use. All other chemicals were employed without further purification: tetrasisopropyl-orthotitanate (TIP) (Merck, 98%), hydrochloric acid (1 M) (Merck), ethylene glycol (EG) (Merck, 99%), Isopar M (Caldic), and acetone (Merck, 99%). P(E/B-b-EO) (MW ∼ 12 000 $g \cdot mol^{-1}$) was prepared by coupling "Kraton liquid" (MW = 3900 g/mol) (ω-hydroxypoly(ethylene-*co*-butylene)) with ethylene oxide by anionic polymerization.[46] Demineralized water was used during the experiments.

Synthesis of the Precursor. EGMT was prepared in a 1 L one-necked Schlenk flask in argon atmosphere by a modified procedure of Xia et al.[15] EG and TIP (molar ratio of 2 to 1) were dissolved in THF and refluxed for 5 h at 90 °C. THF and the isopropyl alcohol released during hydrolysis were distilled off at 120 °C. The precursor was dried under reduced pressure at 170 °C and obtained as a white powder. The resulting EGMT was characterized by thermal gravimetric analysis (TGA): EGMT contained 28.3 wt % Ti (theoretical value: 28.5 wt %).

Synthesis of TiO_2. Porous TiO_2 nanoparticles were prepared by the inverse miniemulsion technique. The amounts of the ingredients are given in Table 1. The dispersed aqueous phase consisting of EGMT, hydrochloric acid (1 M), and ethylene glycol (EG) (V(HCl+EG) = 10 mL) was added to the continuous organic phase containing the surfactant (P(E/B-b-EO)) and Isopar M. The mixture was sonicated in an ice-cooled bath for 6 min (30 s pulse, 10 s pause) at 90% amplitude (Branson sonifier W-450 digital, 1/2 in. tip). The reaction was performed at elevated temperature (20 to 150 °C, see details in text) for 18 h. The particles were recovered by centrifugation and purified by repetitive centrifugation/redispersion using demineralized water and acetone. The resulting TiO_2 was dried in air, followed by calcination at elevated temperature (50 to 1200 °C) for 4 h.

Characterization. The average size of the droplets was measured using a Zetasizer Nano Series (Malvern Instruments, U.K.) at a fixed scattering angle of 173°. DLS measurements give a value called *Z*-average size, which is an intensity average, and the polydispersity index PDI. The standard cumulant analysis is the fit of a polynomial to the log of the G1 correlation function (eq 1).

$$\ln(G1) = a + bt + ct^2 + dt^3 + ... \quad (1)$$

The value of second order cumulant b is converted to a size using the dispersant viscosity and some instrumental constants. The

(43) Zhang, S.; Yu, Q.; Chen, Z.; Li, Y.; You, Y. *Mater. Lett.* **2007**, *61*, 4839.
(44) Thoms, H.; Epple, M.; Fröba, M.; Wongb, J.; Reller, A. *J. Mater. Chem.* **1998**, *8*, 1447.
(45) Khushalani, D.; Dag, O.; Ozin, G. H.; Kuperman, A. *J. Mater. Chem.* **1999**, *9*, 1491.
(46) Thomas, A.; Schlaad, H.; Smarsly, B.; Antonietti, M. *Langmuir* **2003**, *19*, 4455.

coefficient of the squared term c, when scaled as $2c/b^2$, is known as the polydispersity or polydispersity index (PDI). The calculations for these parameters are defined in the ISO standard document 13321:1996 E.

The particle size and morphology was observed by transmission (TEM, Philips EM 400T) and scanning electron microscopy (SEM, Zeiss DSM 962 instrument). The TiO_2 powders were dispersed in acetone, and one drop was placed on a carbon-coated copper grid for TEM and on an aluminum plate for SEM. The samples were dried at room temperature, and with TEM, the grid was examined at an accelerating voltage of 80 kV without additional contrasting. Before examination with SEM the aluminum plates were sputtered with Pd/Au.

High resolution TEM and analytical TEM samples were embedded in epoxy. HRTEM for the structural characterization was performed at a Philips CM20 operating at 200 kV. Energy filtered TEM (EFTEM) was performed at a Cs-corrected Titan 80−300 equipped with a Gatan energy filter and operated at 300 kV to obtain elemental mappings.

The crystalline phase was identified by X-ray diffraction (XRD) using Cu Kα radiation ($\lambda = 0.154$ nm) on a PANalytical XPert Pro. The crystallite size was calculated from XRD measurements by the Scherrer equation. For in situ measurements of the heat treatment, a HT chamber TCU 1000N was applied.

The specific surface area of the particles was determined by nitrogen sorption experiments on a NOVA 4000e or Autosorb MP1 instrument (Quantachrome). The surface area was calculated by the 5-point method according to Brunauer, Emment and Teller (BET) in the p/p_0 range of 0.05−0.3. Prior to the measurement, the samples were degassed at 150 °C for 3 h in vacuo.

Results and Discussion

For the synthesis of porous titania nanoparticles, a glycol-modified precursor (bis(2-hydroxyethyl)titanate, EGMT) was used. By hydrolysis and condensation in aqueous media TiO_2 is formed under release of ethylene glycol. The advantages of glycol-modified precursors are their water solubility in acidic medium and their relatively slow hydrolysis compared to commercially available titanium alkoxides. This allows convenient handling also in inverse miniemulsion. For the synthesis, the precursor (EGMT) was dissolved in hydrochloric acid and dispersed in a mixture of hydrocarbons (Isopar M). By homogenization with ultrasound small monodisperse droplets were formed in which hydrolysis of the precursor and subsequent condensation to the final TiO_2 nanoparticles takes place. As surfactant an amphiphilic block copolymer (P(E/B-b-EO)) was used, which stabilizes the droplets sterically, thus preventing droplet collision and coalescence. This block copolymer is the only surfactant used in this synthesis. Generally, the benefit of the miniemulsion technique is the possibility of controlling the final particle size by the amount of surfactant. Every droplet acts as independent nanoreactor, which means there is no change in droplet size, droplet number, and concentration in each droplet during the reaction.

In this work, we investigated the effects of synthesis conditions on droplet and particle size, porosity, crystallite size, crystallite phase, and specific surface area. There are several possibilities to modify the final material. At first, the composition of the dispersed phase can be changed by varying the molar ratio of the precursor (EGMT) to hydrochloric acid and the use of a mixture of hydrochloric acid and ethylene glycol as dispersed phase. Second, the synthesis temperature can be varied to modify the hydrolysis reaction rate. Moreover, the final particle size can be easily tuned by the droplet size and therefore by the amount of surfactant (P(E/B-b-EO)).

Finally, after synthesis the as-synthesized TiO_2 can be calcined at different temperatures. For characterization of the obtained TiO_2 dynamic light scattering (DLS), transmission (TEM) and scanning electron microscopy (SEM), X-ray diffraction (XRD), and nitrogen sorption (BET) were used.

Variation of the Composition of the Dispersed Phase. An important parameter in controlling the hydrolysis reaction rate is the amount of water with respect to the precursor. The water content determines the initial species formed during hydrolysis and therefore strongly influences the resultant phase produced. Generally, at higher pH the crystallization of anatase is favored, whereas at lower pH rutile is usually formed.[47,48] If the pH is not high enough for direct crystallization of anatase or low enough for direct crystallization of rutile, kinetic factors have to be taken into account. In this case the final crystalline material might result of recrystallization of an intermediate phase.[47] Here we used an aqueous acidic medium which favors the hydrolysis reaction versus the condensation reaction.[12]

In acidic (HCl) media Ti^{4+} ions hydrolyze spontaneously. They are octahedrally coordinated with ligands such as Cl^-, OH^-, and H_2O. The amount of OH^- is determined by the pH value of the system. The complex ion $[Ti(OH)_x Cl_y(H_2O)_z]^{4-x-y}$ ($x + y + z = 6$) seems to exist in the beginning hydrolysis step. At low pH there are only few OH^- groups bound to the Ti center. With increasing temperature the hydrolysis of $[Ti(OH)_x Cl_y(H_2O)_z]^{4-x-y}$ is accelerated and the Cl^- ligands are replaced by water molecules to form $-Ti-OH_2$. The hydroxylated species is the precursor for the final condensation product. By oxolation (dehydration) of two hydroxyl groups of different $[Ti(OH)_x(H_2O)_{6-x}]^{4-x}$ complexes, Ti−O−Ti bridges can be formed. At the beginning of the condensation the dimer $[Ti_2(OH)_8(H_2O)_2]$ is created. In this complex both octahedra share one edge. The number and size of the primary particles depend on the relative nucleation and growth rates. By further condensation through oxolation crystallization to anatase or rutile might start. In rutile two opposing edges of TiO_6 octahedra are connected to build linear chains which are linked via corners. In anatase each TiO_6 octahedron shares four edges, thus forming zigzag chains which are linked by edges. Consequently, in anatase four edges per octahedron are shared but in rutile only two.[48−50] As described above the nucleation process determines the crystalline phase which is formed. The final particle size is generated by growth.

With a constant amount of surfactant (0.7 wt % (P(E/B-b-EO)) with respect to the dispersed phase) and a synthesis temperature of 100 °C, the ratio of EGMT to hydrochloric

(47) Li, J.-G.; Ishigaki, T.; Sun, X. *J. Phys. Chem. C* **2007**, *111*, 4969.
(48) Jolivet, J.-P. *Metal Oxide Chemistry and Synthesis From Solution to Solid State*; Wiley: Chichester, 2000.
(49) Lu, C.-H.; Wen, M.-C. *J. Alloys Compd.* **2008**, *448*, 153.
(50) Cheng, H.; Ma, J.; Zhao, Z.; Qi, L. *Chem. Mater.* **1995**, *7*, 663.

Table 2. Droplet Sizes and Polydispersity Indices of the Miniemulsions after Ultrasonication and after Heating at 100 °C with Different Amounts of HCl with Respect to EGMT

HCl:EGMT [mol]	average droplet size after ultrasonication [nm]	PDI	average droplet size after heating [nm]	PDI
2.8:1	800	0.204	270	0.061
3.2:1	860	0.276	200	0.090
3.8:1	800	0.235	220	0.023
4.3:1	880	0.354	240	0.134
4.8:1	900	0.355	210	0.083
5.4:1	830	0.304	220	0.059

acid (1 M) in the dispersed phase was varied while the pH value of 0 was not changed.

Table 2 shows the droplet sizes and polydispersity after ultrasonication and after heating at 100 °C for 18 h. With a molar ratio of precursor to hydrochloric acid (1 M) of 1 to 2.7−5.4, all droplet sizes determined by dynamic light scattering (DLS) were in the same size range of 800−900 nm with a polydispersity index of about 0.3 directly after ultrasonication. The different amounts of hydrochloric acid in the dispersed phase did not affect the miniemulsion system. After heating the miniemulsion at 100 °C the droplet sizes and the polydispersity decreased significantly from 800 nm to about 250 nm with a polydispersity index of 0.1 as can be seen in Table 2. As heating the miniemulsion resulted in evaporation of water, the final droplets only contained TiO_2 and ethylene glycol.

Transmission electron micrographs show porous spherical particles between about 100 and 250 nm (Figure 1). These values correspond well with the droplet sizes of about 250 nm determined by DLS after heating the miniemulsion at 100 °C (Table 2). No difference in the particle size with different ratio of hydrochloric acid to EGMT was observed, which is in good agreement with the DLS measured droplet sizes that did not change with different ratios as well. The crystallite size was determined by HRTEM studies (Figure 4a−d) to 5−10 nm in diameter. The crystallites were found to be loosely aggregated, thus forming pores (see also Figure 1).

For the as-prepared material anatase is the only phase that is detected in the X-ray diffraction patterns. However, there are no peaks in the low angle range of patterns indicating the absence of long-range order pore arrangements. Even after calcination at 400 °C for 4 h, where the surfactant has been removed completely (proven by thermal gravimetric analysis (TGA)), porous particles (Figure 1b,c) can be observed beneath loosely aggregated nanocrystallites. The preformed crystalline particles seem to be stable enough to withstand the calcination process with the removal of the surfactant. The temperatures are not sufficiently high to transfer anatase in the thermodynamically stable rutile. BET measurements reveal for this material a specific surface area of as high as 140 $m^2 \cdot g^{-1}$ even after calcination.

Typically, with other techniques and different precursors, an amorphous solid material is formed. There are only few groups that could synthesize crystalline titania at temperatures below 100 °C.[16−24] However, most of the obtained materials are not porous. Therefore the combination of the miniemulsion technique with the slow reacting titanium precursor seems to favor crystallization to porous particles even at lower temperatures due to the high controllability in the droplets. As a result of the suppression of diffusion processes between the droplets which might affect the final particle size, an orientation process within the droplet is favored.

Usually macrocrystalline rutile is thermodynamically more stable than macrocrystalline anatase and brookite. However, the final product is not necessarily thermodynamically stable and depends on acidity, precursor concentration, and temperature of the system. If a material has several crystalline phases, a metastable phase usually precipitates first which might be transformed, for example, during aging into the stable phase. The explanation for this lies in kinetic effects.[48]

Another important factor is that the thermodynamic stability depends on the particle size. Below a critical particle diameter of approximately 14 nm, the total free energy of rutile is higher than that of anatase and the relative phase stability of rutile and anatase reverses.[11] Therefore, anatase is more stable than rutile at very small particle diameters. As the activation energy of phase transformation is related to the particle size, the critical particle size varies slightly with temperature because a change in temperature changes the kinetic energy of atoms in the nanocrystalline anatase. This phenomenon is called quantum size effect.[11]

The TiO_2 phase composition after calcination was analyzed in detail by XRD (Figure 2). It can be observed that it changed with different amounts of hydrochloric acid. Whereas the molar ratio of EGMT to HCl of 1 to 5.4 produced a pure anatase phase, with decreasing amount of hydrochloric acid rutile was additionally formed as can be seen in the XRD pattern in Figure 2. It shows peaks attributed to rutile (*) which become sharper and more intense with decreasing excess of hydrochloric acid and after calcination at 400 °C. With the diffraction peak intensities of anatase and rutile the weight fraction of rutile could be calculated:

$$\chi = \frac{1}{1 + 0.8\frac{I_a}{I_r}} \tag{2}$$

where χ is the weight fraction of rutile, I_a is the diffraction peak intensity of anatase (101) plane (#), and I_r is the diffraction peak intensity of rutile (110) plane (*).[51] It could be shown that the samples contained constantly about 20 wt % rutile and 80 wt % anatase with a smaller molar ratio of HCl to EGMT than 5.4:1.

Several groups found that in hydrochloric acid media either rutile or anatase can be produced.[52,53] A mixture of anatase and rutile was synthesized with less than 1 M HCl and pure rutile with more than 1 M HCl with hydrothermal treatment.[52] In an acidic system anatase is supposed to form initially. As the surface groups are protonated (Ti-OH_2) TiO_2 becomes soluble. Then a dissolution−crystallization process (Ostwald ripening) takes place because of the higher solubility of the oxide. This transformation is favored by very high

(51) Kim, C.-S.; Kwon, I.-M.; Moon, B. K.; Jeong, J. H.; Choi, B.-C.; Kim, J. H.; Choi, H.; Yi, S. S.; Yoo, D.-H.; Hong, K.-S.; Park, J.-H.; Lee, H. S. *Mater. Sci. Eng. C* **2007**, *27*, 1343.
(52) Wu, M.; Long, J.; Huang, A.; Luo, Y. *Langmuir* **1999**, *15*, 8822.
(53) Calleja, G.; Serrano, D. P.; Sanz, R.; Pizarro, P.; García, A. *Ind. Eng. Chem. Res.* **2004**, *43*, 2485.

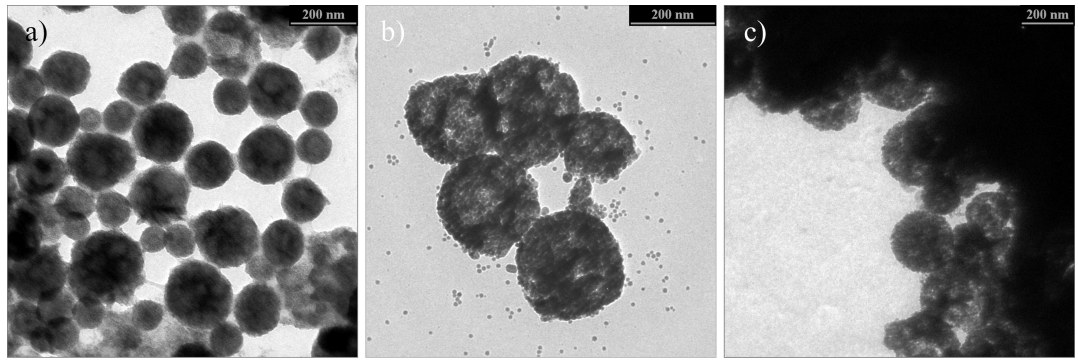

Figure 1. TEM images of TiO_2 nanoparticles prepared at 100 °C with molar ratios: (a) EGMT:HCl = 1:5.4 as synthesized, (b) EGMT:HCl = 1:3.2 after calcination at 400 °C, and (c) EGMT:HCl = 1:4.3 after calcination at 400 °C.

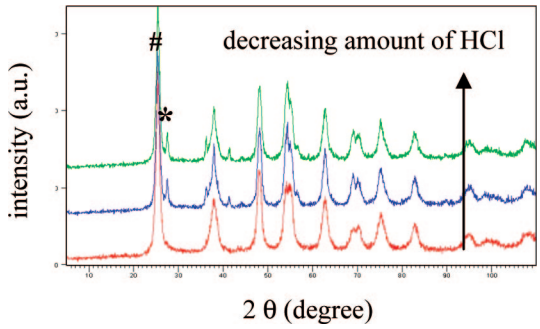

Figure 2. XRD patterns of TiO_2 nanoparticles synthesized with different amounts of HCl with respect to EGMT (after calcination at 400 °C): HCl:EGMT = 2.8:1 (green line), HCl:EGMT = 3.8:1 (blue line), HCl:EGMT = 5.4:1 (red line); # marks the anatase (101) peak, * the rutile (110) peak.

acid content and high temperatures. Consequently, the final crystalline phase is rutile which is thermodynamically more stable.[48,48,54]

In our work we could synthesize both a mixture of both phases and pure anatase with 1 M HCl. However, this can be attributed to the obvious differences between our synthesis method compared to the literature mentioned above. Consequently, the crystalline phase composition of TiO_2 can be easily adjusted by the amount of hydrochloric acid. To obtain pure anatase the molar ratio HCl to EGMT of 5.4:1 has to be employed.

Another possibility of reducing the amount of water and therefore controlling the hydrolysis reaction rate is to use a mixture of hydrochloric acid (1 M) and ethylene glycol (EG) without changing the total volume of the dispersed phase.[15] With a constant amount of surfactant (0.7 wt % P(E/B-b-EO) compared to the dispersed phase), a synthesis temperature of 100 °C and a volume ratio of HCl to EG of 1:1 and 1:4, spherical porous particles between 90 and 350 nm as revealed by TEM (see Figure 3a) with a larger size distribution than for the samples prepared without additional EG were obtained. As ethylene glycol is not as hydrophilic as hydrochloric acid, it has a slightly higher solubility in the continuous phase. Whereas before the reaction it is expected to be a compensative diffusion (principle of miniemulsion is fulfilled!), throughout the reaction hydrolysis and condensation in the different droplets can proceed differently leading to changes in the osmotic pressures between the droplets resulting in a diffusion of material through the continuous phase and consequently in a change in the droplet size distribution and finally the particle size distribution.[34] Therefore, the initially homogeneous droplets change in size distribution during reaction and form particles with a broader size distribution.

As it can be seen from the XRD data in Figure 3b, the samples consist of pure anatase. By applying the Scherrer equation on the (101) diffraction peak of anatase (#), the average crystallite size was estimated to be about 10 nm in size. Investigations with scanning electron microscopy (Figure 3c) and TEM (Figure 3a,d) show that all particles are spherical in morphology and have a relatively narrow size distribution. HRTEM investigations revealed that the particles are composed of nanocrystallites (see Figure 4 b−d).

TEM investigations on the particles which are embedded in epoxy resin clearly showed that the particles are compartmented (see Figure 4a−d). The survey in Figure 4a shows that the compartments vary in size and number per particle. The particles are built-up of TiO_2 nanocrystallites and an amorphous matrix. Figure 4 d shows the inner part of a single particle from Figure 4a,b. The TEM micrographs of the inner compartments clearly show that they are filled with an amorphous matrix and TiO_2 nanocrystallites. Figure 4c shows a TEM image of the shell interface between the framework and the inner compartment of the particle in Figure 4b. It can clearly be seen that the crystalline shell is porous. The crystallite size varies between 5 and 10 nm diameter. The amorphous matrix is present in the whole particle. Further investigations with elemental mappings by energy filtered TEM (see Figure 4 e−g) revealed that the particles are composed of titania nanocrystallites. The amorphous matrix, which surrounds the titania nanocrystallites, is clearly composed of carbon that either originates from the embedding epoxy or from the residual glycol and/or the surfactant from the synthesis.

Besides the small amount of amorphous material it could be shown that the particles consisted mostly of nanocrystalline TiO_2 which aggregated to form porous particles. A reason for the significant difference in density inside the particles might be the additional amount of EG in the dispersed phase. Larger amounts of EG seem to favor the phase separation of TiO_2 and EG leading to particles with

(54) Yanagisawa, K.; Ovenstone, J. *J. Phys. Chem. B* **1999**, *103*, 7781.

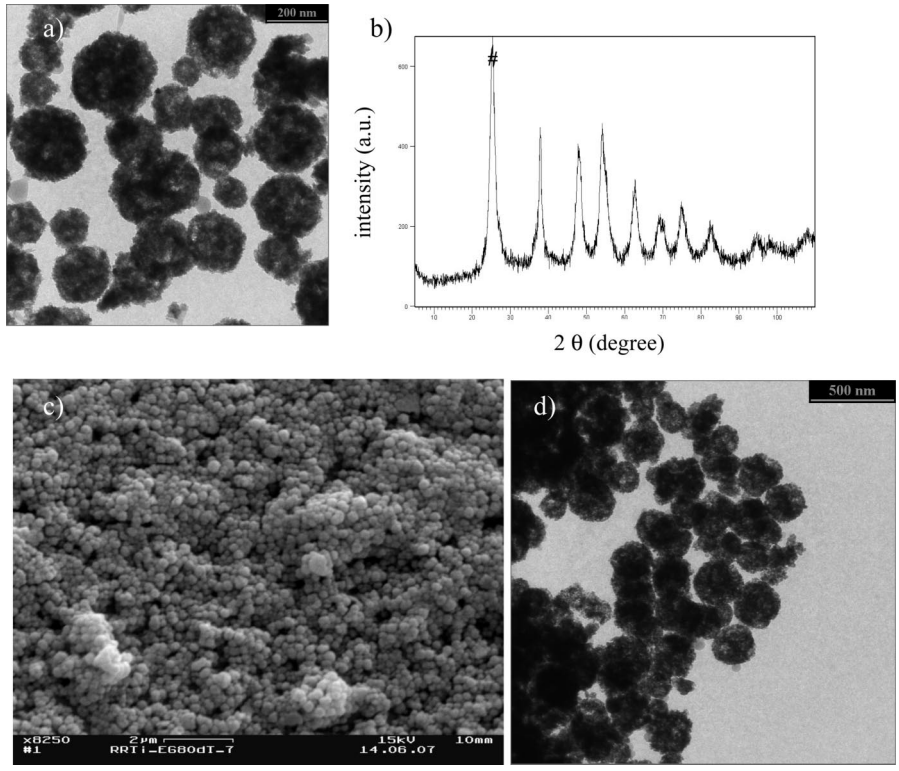

Figure 3. (a) TEM image of as-synthesized porous titania nanoparticles (at 100 °C with ethylene glycol); (b) XRD pattern of as-synthesized TiO_2 nanoparticles (# marks the anatase (101) peak); (c) SEM image of as-synthesized titania nanoparticles; and (d) TEM image of porous titania particles after calcination at 400 °C.

differences in density. Figure 3d shows a TEM image of TiO_2 particles after calcination at 400 °C. In comparison to the synthesis without additional ethylene glycol in the dispersed phase, the spherical morphology of these aggregated colloidal particles was completely preserved even after thermal treatment at 400 °C for removal of the surfactant. Although still high, the specific surface area determined by BET measurements did not exceed the value of 120 $m^2 \cdot g^{-1}$ obtained with a molar ratio of HCl to EGMT of 5.4:1 and without additional ethylene glycol.

In summary, the composition of the dispersed phase affects the phase composition and the internal particle structure of the final TiO_2 material.

Variation of the Synthesis Temperature. In further studies the influence of the synthesis temperature on the crystallite phase composition of the resulting TiO_2 was examined. The synthesis temperature influences the rate of the hydrolysis and condensation reaction and therefore might change the crystallite phase and size.

In the following experiments the range of temperatures was varied between 20 and 150 °C with a constant amount of surfactant (0.7 wt % P(E/B-b-EO)) and EGMT with respect to HCl (1 to 5.4 (mole ratio)).

Table 3 shows the droplet sizes and polydispersity indices of the miniemulsions before and after heating at different temperatures. As the different samples only differ in the heating temperature, the droplet sizes after ultrasonication were all about 800 nm with a polydispersity index of about 0.3. After heating for 18 h, the droplet sizes decreased significantly as described in the previous paragraph to values of about 200 nm. Only the sample prepared at 20 °C did not change in size since the water could not evaporate. All miniemulsions apart from the sample prepared at 150 °C were stable dispersions after heating.

Figure 5a shows the XRD patterns of as-synthesized titanium dioxide obtained at different reaction temperatures. As can be seen at room temperature amorphous TiO_2 was obtained. With increasing temperature a mixture of rutile (*) and anatase (#) was synthesized, and only at temperatures above 100 °C selectively anatase was formed. By employing the Scherrer equation the crystallite sizes of the samples prepared at 75, 100, and 150 °C could be calculated to be in the same size range of about 5 nm.

After calcination at 400 °C (see Figure 5b) the samples synthesized at room temperature, 100 °C, and 150 °C contained pure anatase. Calcination of the samples prepared at 50 and 75 °C led additionally to the formation of rutile. By calcination, all peaks became sharper indicating an increasing crystallite size which could be calculated (using the Scherrer equation) to be of about 9 nm for all samples.

Watson et al. also examined the crystalline phases synthesized at different temperatures and produced rutile at lower temperatures as well. Between 60−75 °C rutile was formed, whereas at 90 °C a mixture of anatase and brookite was obtained.[55]

Kim et al. showed that a crucial factor for crystallinity is the reaction temperature.[25] They also synthesized a crystalline material below 100 °C. Using $TiCl_4$ and acidic media they obtained pure rutile below 65 °C, pure anatase at 100 °C, and a mixture of both in between. With this method a specific surface area of 148 $m^2 \cdot g^{-1}$ was reported, and the anatase

(55) Watson, S.; Beydoun, D.; Scott, J.; Amal, R. *J. Nanopart. Res.* **2004**, *6*, 193.

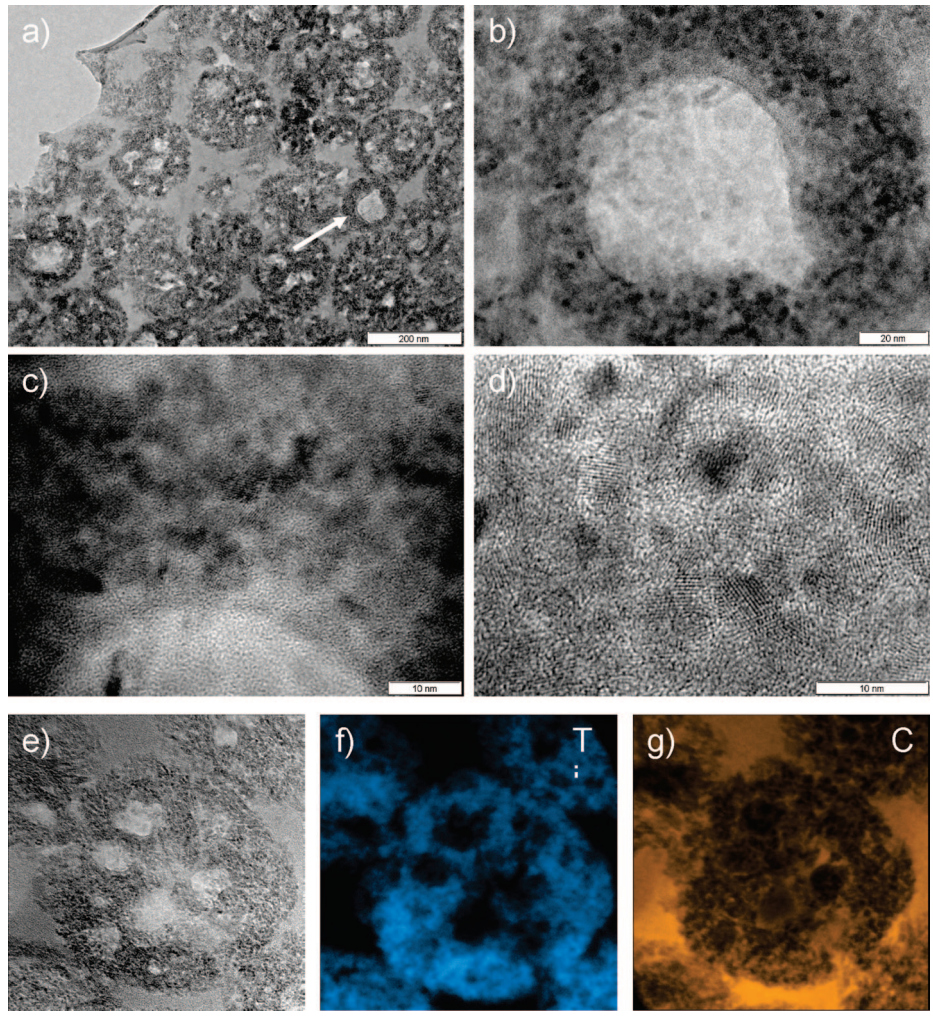

Figure 4. HRTEM micrographs of as-synthesized porous titania nanoparticles (100 °C with EG). The particles are embedded in epoxy. (a) Survey of the sample. Arrow points to a particle chosen for closer investigation. (b) The particle shows a high crystallite density in the rim and a low crystallite density in the center. (c) HRTEM micrograph shows that the rim consists of nanocrystallites. (d) HRTEM micrograph shows that the core consists of nanocrystallites. (e) Zero-loss image of a single particle. (f) Ti EFTEM map shows that the crystallites are composed of Ti. (g) C EFTEM map shows that the carbon is localized inbetween the titania nanocrystallites and inbetween the particles.

Table 3. Droplet Sizes and Polydispersity Indices of the Miniemulsions after Ultrasonication and after Heating at Different Temperatures

temperature of preparation [°C]	average droplet size after ultrasonication [nm]	PDI	droplet size after heating [nm]	PDI
20	790	0.341	830	0.261
50	830	0.278	240	0.073
75	810	0.300	220	0.045
100	840	0.304	220	0.059
150	820	0.312		

particles of 2−5 μm consisted of 10 nm primary particles. They also observed a reversed phase formation. The authors explain this with a different reaction rate. Higher reaction temperatures result in anatase which is energetically more favored at these temperatures. Rutile can be formed at lower temperatures because the reaction rate is low enough to result in stable crystallites below 100 °C. This means that the difference lies in the reaction rate which depends on the reaction temperature and which determines if an energetic or thermodynamic product is formed.[25]

Here, similar to the results mentioned above, it is possible to control the crystalline phase composition without calcination, but with the adjustment of the synthesis temperature. With temperatures below 150 °C it is possible to synthesize crystalline materials without a significant growing of the crystallites usually induced by calcination. Samples with pure anatase could be prepared with and without calcination, but only without calcination the small crystallite size of 5 nm could be preserved (synthesized at 100 or 150 °C). Therefore heat treatment at relatively low temperatures compared to calcination at high temperatures favors small crystallite sizes and avoids significant crystallite coarsening.

Another explanation for the formation of anatase at temperatures above 100 °C might be the dissolution−crystallization process. As already mentioned the final product is not necessarily thermodynamically stable and depends on acidity, precursor concentration, and temperature of the system. In an acidic system anatase usually precipitates first. The explanation for this lies in kinetic effects.[48] The synthesis of rutile is proposed to be a dissolution−crystallization of anatase. However, in the absence of solvent (100 °C) this transition to rutile cannot take place which can be compared to hydrolysis in vapor phase where only anatase is formed. The synthesis of anatase in solution is strongly influenced

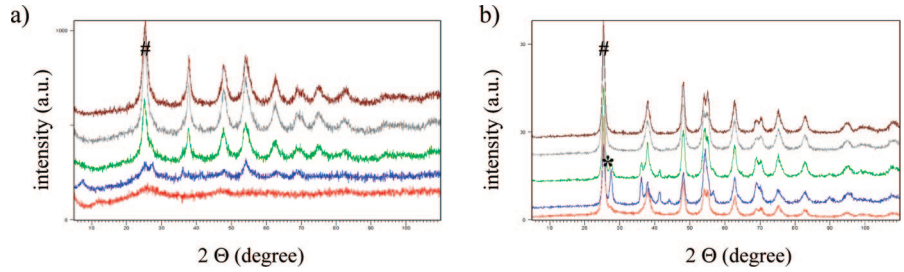

Figure 5. XRD patterns of TiO_2 nanoparticles synthesized at room temperature (red line), 50 °C (blue line), 75 °C (green line), 100 °C (gray line), and 150 °C (brown line) (a) as-synthesized and (b) after calcination at 400 °C; # marks the anatase (101) peak, * the rutile (110) peak.

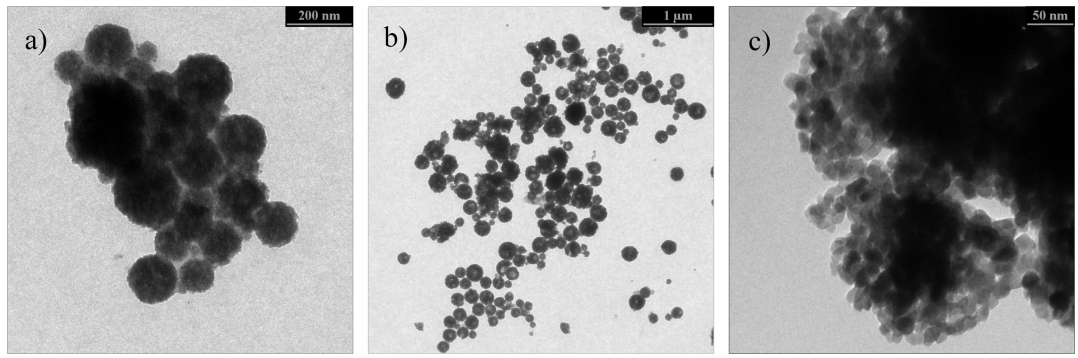

Figure 6. TiO_2 nanoparticles synthesized at different temperatures: (a) 75 °C (as-synthesized), (b) 150 °C (as-synthesized), and (c) 75 °C (after calcination at 400 °C).

Table 4. Droplet Sizes and Polydispersity Indices of the Miniemulsions after Ultrasonication and after Heating with Different Amounts of Surfactant ((P(E/B-b-EO) with Respect to the Dispersed Phase)[a]

amount of P(E/B-b-EO) [wt %]	average droplet size after ultrasonication [nm]	PDI	average droplet size after heating [nm]	PDI	crystallite size [nm]	specific surface area [m^2/g]
0.7	940	0.311	220	0.059	8	141
1	900	0.459	180	0.041	7	118
2	560	0.592	110	0.062	6	208
5	340	0.396	70	0.184	5	321

[a] The crystallite size of the final materials was calculated by Scherrer equation, and the specific surface area was determined by nitrogen sorption (BET).

by kinetic (rate of precipitation) and thermodynamic (solubility) effects.[48]

Comparing the two samples prepared above 100 °C (100 and 150 °C) they only differ in their particle size distribution determined by TEM analysis. For the reactions at 100 °C and below, spherical particles of 100 to 200 nm can be observed in the TEM images (Figure 1a and Figure 6a, as-synthesized) whereas a size of 70 to 320 nm is detected for particles prepared at 150 °C (Figure 6b). The variation in the size distribution can be explained with a different evaporation process at the different temperatures. With heating the miniemulsion at 150 °C, water will evaporate faster leading to a rapid change in droplet size compared to synthesis at 100 °C. Therefore, the droplet size and consequently the particle size distribution might be affected. After calcination loosely aggregated crystallites could be observed for both (but also the other) temperatures after synthesis (Figure 6c).

In conclusion, it could be shown that the TiO_2 phase composition can be easily changed by variation of the synthesis temperature. Moreover, small crystallites can be obtained and preserved without coarsening, which is typically caused by calcination at temperatures higher than 350 °C. As anatase nanoparticles are preferred for many applications, a temperature of 100 °C has to be chosen, where pure anatase with relatively narrow size distribution before (ca. 5 nm) and after calcination (ca. 9 nm) could be synthesized.

Variation of the Amount of P(E/B-b-EO). In a next set of experiments, the amount of surfactant (P(E/B-b-EO)) used for the stabilization of the miniemulsion was varied and the influence on the crystallite size and especially on the specific surface area was investigated. For the miniemulsion technique the concentration of surfactant is a crucial factor. By varying the amount of surfactant with respect to the dispersed phase, the droplet size can usually be adjusted over a wide range. Table 4 shows the droplet sizes after ultrasonication and after heating with different amounts of surfactant at a constant molar ratio of EGMT to HCl (1:5.4) and at a synthesis temperature of 100 °C. As it can be seen, the droplet size decreased as expected with increasing amount of surfactant. Whereas the droplet diameter is about 900 nm with 0.7 wt % of P(E/B-b-EO) (with respect to the dispersed phase) after ultrasonication, the size decreased to 350 nm with 5 wt % of P(E/B-b-EO). Comparing the droplet sizes after heating the miniemulsions, the droplet diameters also decreased with increasing amount of surfactant. With 5 wt % of P(E/B-b-EO) a value as low as 70 nm was obtained. Comparing the change in droplet diameter before and after

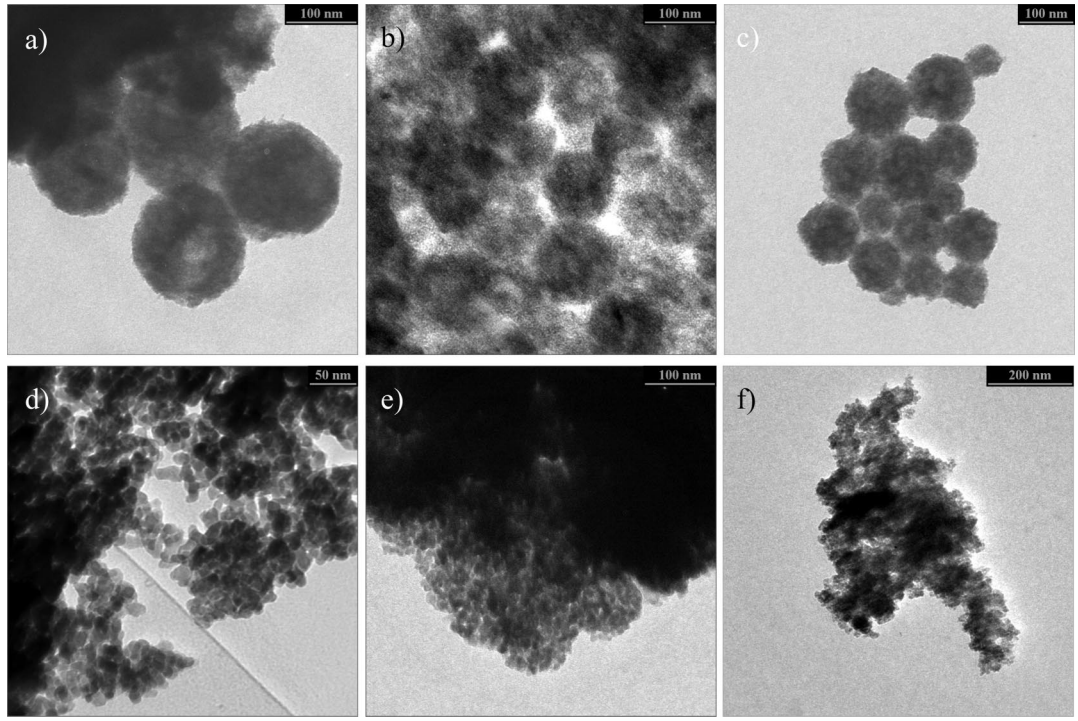

Figure 7. TEM images of anatase crystallites synthesized with different amount of surfactant: (a) 0.7 wt % P(E/B-b-EO) (as-synthesized), (b) 0.7 wt % P(E/B-b-EO) (as-synthesized) embedded in epoxy resin, (c) 1 wt % P(E/B-b-EO) (as-synthesized), (d) 0.7 wt % P(E/B-b-EO) after calcination at 400 °C, (e) 1 wt % P(E/B-b-EO) after calcination at 400 °C, and (f) 5 wt % P(E/B-b-EO) after calcination at 400 °C.

heating, all samples decreased to about 20% of the initial droplet diameter. In principle, all droplets in a miniemulsion are similar in size and contain the reactants in the same concentration. Consequently the same amount of water is removed by evaporation of the water. In the case of different miniemulsions with different droplet sizes the same percentage of water will be removed.

Figure 7 shows some TEM images of anatase crystallites and particles synthesized with different amounts of surfactant (P(E/B-b-EO)). The as-synthesized crystallites aggregate to spherical porous particles which are obtained independent of the surfactant amount (Figure 7a-c). The sizes of the spherical particles decreased from 150 to 50 nm with increasing surfactant amount. In a miniemulsion the surfactant is located at the interface between the aqueous and continuous phase, which means on the droplet surface. With increasing amount of surfactant, a higher interface and therefore smaller droplets can be stabilized. Consequently, the resulting titania particles, which are formed directly out of the droplets, are smaller as well.

Figure 7b shows particles synthesized with 0.7 wt % P(E/B-b-EO) embedded in epoxy resin. Compared to the particles synthesized with additional ethylene glycol (EG) as the dispersed phase (Figure 4), the significant difference in density between the edge and the inner part of a particle cannot be observed for these particles. As the only difference in synthesis is the amount of ethylene glycol, bigger amounts of EG seemed to favor the phase separation of TiO_2 and EG leading to particles with differences in density. Comparing the results obtained by TEM analysis, the particles synthesized without additional EG seem to be more homogeneous than those prepared with additional EG.

After thermal treatment at 400 °C to remove the surfactant (complete removal could be proven by TGA), the crystallites were still aggregated, but the shape was not spherical anymore (Figure 7d−f) for the samples synthesized with more than 1 wt % P(E/B-b-EO). Comparing the aggregation behavior before and after calcination indicates that the surfactant influences the aggregation of the crystallites. As the surfactant is located at the interface between aqueous and organic phase and its hydrophilic poly(ethylene oxide) chains are partly inside the aqueous droplets, there might be some interactions between the titania species and the block copolymer. Pore size distributions determined by BJH showed that the values are about 10 nm after calcination at 400 °C. This size range is similar to that reported by Smarsly et al.[56] They already used this poly(ethylene oxide)-based surfactant for structure formation in the synthesis of porous silica. As interactions hydrogen bonding between the poly(ethylene oxide) chains of the surfactant and the precursor are suggested to direct the structure formation. Thus, it might be possible to induce pore formation in the titania even at an elevated temperature of 100 °C without the addition of another surfactant. This means that the amphiphilic block copolymer used for the stabilization of the miniemulsion causes the porous nature of the anatase nanoparticles. After centrifugation of the miniemulsion and washing the sample with water and acetone, the surfactant is partly removed. The remaining part is still attached to the particle surface, and might be moving inside the particle between the crystallites leading to the aggregated structure. After calcination, the surfactant is removed completely (proven by TGA) and no

(56) Smarsly, B.; Grosso, D.; Brezesinski, T.; Pinna, N.; Boissiere, C.; Antonietti, M.; Sanchez, C. *Chem. Mater.* **2004**, *16*, 2948.

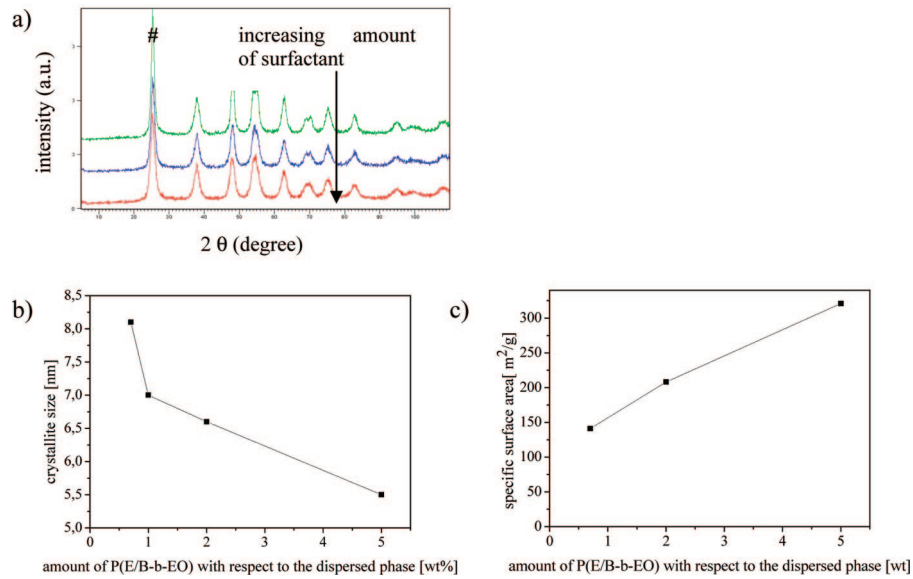

Figure 8. Different parameters in dependence on the amount of surfactant (P(E/B-b-EO)): (a) XRD patterns of titania nanoparticles (after calcination at 400 °C) with 0.7 wt % P(E/B-b-EO) (green line), 2 wt % P(E/B-b-EO) (blue line), and 5 wt % P(E/B-b-EO) (red line), # marks the anatase (101) peak; (b) correlated size average of anatase crystallites calculated by Scherrer equation; and (c) specific surface area determined by nitrogen sorption (BET).

spherical particles could be observed by TEM analysis for the samples synthesized with more than 1 wt % P(E/B-b-EO) (Figure 7d−f). The crystallites are aggregated without forming any special shape. The reason for this lies in the amount of surfactant which has to be removed by calcination. For 0.7 wt % and 1 wt % P(E/B-b-EO) only a small quantity of surfactant per particle has to be removed after washing, thus not changing the particle morphology drastically. If higher amounts of P(E/B-b-EO) have to be removed, the system is changed strongly, thus leading to a different mophology.

As seen from the XRD data in Figure 8a, all samples contained exclusively anatase already as-synthesized and after surfactant removal by calcination at 400 °C. The reflections in the different XRD patterns (Figure 8a) became broader with increasing amount of surfactant. By applying the Scherrer equation on the (101) diffraction peaks of anatase (#) the crystallites with 0.7 wt % P(E/B-b-EO) were estimated to be 8 nm in size and with 5 wt % P(E/B-b-EO) of about 5 nm (Figure 8b). The change in crystallite size might be related to the presence of the surfactant. The hydrophilic part of P(E/B-b-EO) is likely to interact with the nanoparticle surface and moreover with the crystallite surface thus providing additional sterical stabilization. To determine whether the surfactant is built into the colloidal particles, EFTEM (on the particles shown in Figure 4) and XRD measurements were performed before the calcinations step. EFTEM measurements showed that the particles contain also inside carbon (see previous paragraph) which might be residues from the surfactant. XRD measurements prove the small crystallite size even after calcination. This indicates that the surfactant around the primary crystallites prevents the formation of larger particles. Therefore, we assume that the surfactant is built into the final particles during the aggregation process. This suggests that after surfactant removal the particles are porous with high specific surface area.

With increasing amounts of surfactant, the specific surface area determined by nitrogen sorption (BET) increased significantly. Figure 8c shows the values for the specific surface area in dependence on the amount of surfactant (P(E/B-b-EO)). With 0.7 wt % P(E/B-b-EO) after calcination at 400 °C a specific surface area of 140 $m^2 \cdot g^{-1}$ could be obtained. With increasing surfactant concentration the specific surface area could be more than doubled with 5 wt % P(E/B-b-EO) to a value higher than 300 $m^2 \cdot g^{-1}$ after calcination. The extremely high specific surface area makes this material interesting for applications in photocatalysis as the photocatalytic activity increases with increasing specific surface area.

Influence of the Calcination Temperature. After repeated extraction of the as-synthesized TiO_2, a calcination step can be added to remove the surfactant completely. To investigate the change in phase composition with increasing calcination temperature, the as-synthesized anatase sample (synthesized at 100 °C with 0.7 wt % P(E/B-b-EO) and EGMT to HCl of 1:5.4 (mol)) was gradually heated up to 1200 °C in air while determining the crystalline phase with X-ray diffraction (XRD).

Figure 9a shows the XRD pattern of as-synthesized TiO_2. It displays all the major peaks of anatase indicating that the sample consisted of pure anatase. Thermal treatment at 400 °C (Figure 9b, blue line), which is the usually employed temperature for calcination in order to remove the surfactant (P(E/B-b-EO)), did not have significant effects on the diffraction patterns of the samples, showing that the anatase phase was retained at this temperature and no phase transformation has occurred. However, the peaks became sharper and more intense, indicating a slight increase of the crystallite size from about 6 nm to about 8 nm (by applying the Scherrer equation on the (101) diffraction peak of anatase (#) and the (110) diffraction peak of rutile (*) as described in the previous paragraph). At about 500 °C, diffraction peaks of rutile also appeared indicating the

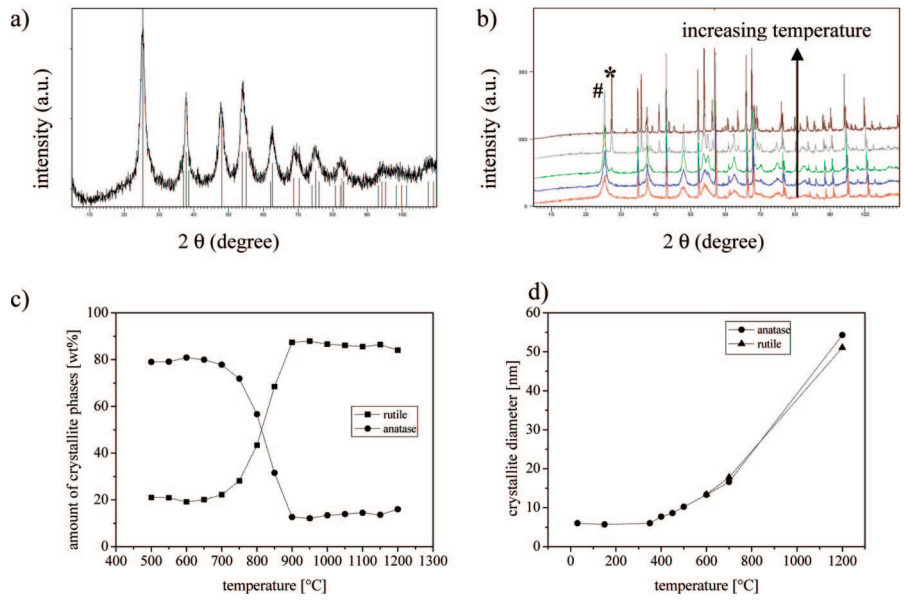

Figure 9. (a, b) XRD patterns of anatase nanoparticles of the as-synthesized sample (a) and with increasing calcination temperature (b): 50 °C (red line), 400 °C (blue line), 500 °C (green line), 750 °C (gray line), and 1200 °C (brown line) (the sharp peaks belong to the sample holder which consisted of aluminum oxide); # marks the anatase (101) peak, * the rutile (110) peak; (c) weight fraction of anatase and rutile with increasing temperature; and (d) correlated crystallite sizes of anatase and rutile with increasing calcination temperature (calculated by the Scherrer equation).

beginning phase transition to rutile which is formed by nucleation and growth by the rearrangement of the octahedra as described above.[22,57] Comparing the XRD patterns at different temperatures it is obvious that the amount of rutile increased with increasing temperature. With the diffraction peak intensities of anatase (101) (#) and rutile (110) (*) the weight fraction of rutile was calculated (Figure 9c) in dependence of the calcination temperature. As it can be seen, the weight fraction of rutile was about 20% at an annealing temperature of about 500 °C, whereas the remaining 80% was anatase. The amount of rutile did not change significantly until 700 °C. Then it increased rapidly to an amount of about 85 wt % until 900 °C. At this temperature the final composition was reached and did not change up to 1200 °C.

The crystallite sizes of the as-synthesized sample were estimated to be about 6 nm in size (Scherrer equation) at room temperature (Figure 9d). During growth of the anatase nanocrystallites with increasing temperature, a phase transition from anatase to rutile occurred at a critical size of about 14 nm in diameter.[11,58] This experimental value agrees well with the theory as described in the previous paragraph. Therefore, a mixture of anatase and rutile is finally obtained after heating at 1200 °C with similar crystallite sizes of about 50 nm. With this synthesis and calcination conditions it is possible to obtain anatase particles even bigger than 14 nm in size, which can be partly preserved until 1200 °C. Comparing the results shows that with heat treatment up to 400 °C (which is the usually employed temperature for calcination in order to remove the surfactant) the sample consisted of pure anatase which is the catalytically most active TiO_2 phase. Moreover, the crystallite size only slightly increased during calcination in this temperature regime. This size is of importance because the band gap of semiconductor nanomaterials increases with decreasing crystallite size. Consequently the absorption edge moves to higher energy; this is the so-called quantum size effect.[59] Thus the photocatalytic activity of anatase increases with small crystallite size and high degree of crystallization.[32] Therefore it is quite important that the crystallites do not grow significantly during calcination to obtain the highest photocatalytic activity.

Conclusions

In summary, a novel template-free approach to synthesize spherical porous anatase particles at a reaction temperature of 100 °C with an average size of about 200 nm was reported. The TiO_2 nanoparticles consist of small anatase crystallites of several nanometers and were prepared by combining sol−gel processing of bis(2-hydroxyethyl)titanate (EGMT) as precursor with the inverse miniemulsion technique.

It was shown that the crystalline phase composition could be easily adjusted by changing the synthesis temperature, varying the ratio of precursor to hydrochloric acid, and using a mixture of hydrochloric acid and ethylene glycol as dispersed phase. While at room temperature only amorphous TiO_2 was formed, with increasing temperature a mixture of anatase and rutile was synthesized and only at temperatures over 100 °C pure anatase was prepared. With different ratio of precursor to hydrochloric acid the crystalline phase composition differed. To obtain pure anatase the molar ratio of precursor to hydrochloric acid of 1:5.4 has to be employed leading to a specific surface area as high as 140 $m^2 \cdot g^{-1}$. With a volume ratio of hydrochloric acid to ethylene glycol of 1:4 as the dispersed phase, the spherical aggregation could be completely preserved after calcination at 400 °C with a specific surface area of about 120 $m^2 \cdot g^{-1}$. However, the particle size distribution increased.

(57) Zhang, H.; Banfield, J. F. *Am. Mineral.* **1999**, *84*, 528.
(58) Gribb, A. A.; Banfield, J. F. *Am. Mineral.* **1997**, *82*, 717.
(59) Zhang, Y.; Li, G.; Wu, Y.; Luo, Y.; Zhang, L. *J. Phys. Chem. B* **2005**, *109*, 5478.

Moreover, it was shown that the crystallite size and therefore the specific surface area can be easily adjusted by the amount of surfactant (P(E/B-b-EO)) which is responsible for stabilizing the miniemulsion. With 5 wt % of surfactant with respect to the dispersed phase the specific surface area could be increased to a value higher than 300 $m^2 \cdot g^{-1}$.

The advantage of this new synthesis approach is the possibility to produce selectively anatase nanocrystals arranged in a spherical manner without any calcination step. Thus, no thermal treatment for crystallization is necessary. Even after calcination at 400 °C for complete removal of the surfactant, a high specific surface area of more than 300 $m^2 \cdot g^{-1}$ can be preserved. This can be very interesting and useful for catalyst supports, for sorption media, and especially in photocatalysis, because the photocatalytic activity increases with increasing specific surface area.

Acknowledgment. Financial support by Deutsche Forschungsgemeinschaft within the Priority Programm (SPP 1181) is gratefully acknowledged. The authors also thank Marlies Fritz for TGA, Conny Egger for BET, and Samuel Blessing for X-ray measurements.

CM800533A